Rare Metal Materials and Engineering
Volume 45, Issue 8, August 2016
Online English edition of the Chinese language journal

Available online at www.sciencedirect.com
ScienceDirect

Cite this article as: Rare Metal Materials and Engineering, 2016, 45(8): 1938-1942.

ARTICLE

Hydrogen Storage Properties of as-Cast $La_{1-x}Sm_xMgNi_{3.6}Co_{0.4}$ (x=0~0.4) Alloys

Zhai Tingting[1,2], Yang Tai[1], Yuan Zeming[1], Xu Sheng[1], Zhang Yanghuan[1]

[1] Central Iron and Steel Research Institute, Beijing 100081, China; [2] Northeastern University, Shenyang 110819, China

Abstract: $La_{1-x}Sm_xMgNi_{3.6}Co_{0.4}$ (x = 0~0.4) alloys were prepared by a vacuum intermediate frequency induction furnace with a high purity helium gas as the protective atmosphere. The effects of partially substituting Sm for La on the phase structure, morphology and hydrogen storage properties of the alloys were investigated. The detections of XRD and SEM reveal that the as-cast alloys contain two phases, $LaMgNi_4$ and $LaNi_5$. The hydrogen storage capacity (wt%) of the alloys decreases with increasing Sm content, namely 1.859, 1.707, 1.585, 1.578 and 1.471, corresponding the variation of x from 0 to 0.4. The P-C-T curves of the alloys show flat plateaus corresponding to the absorption/desorption pressure plateaus of the $LaMgNi_4$ hydride. Meanwhile, the enthalpy change (ΔH) and entropy change (ΔS) of the $LaMgNi_4$ hydrides for hydriding decrease from −40.37 kJ/mol (x=0) to −26.99 kJ/mol (x=0.4) and from −101.9 J (mol/K)$^{-1}$ (x=0) to −77.56 J (mol/K)$^{-1}$ (x=0.4), respectively. The electrochemical measurement displays that the maximum discharge capacity of the alloy electrodes declines from 347 mAh/g to 270.5 mAh/g, which is similar to the trend of the gaseous hydrogen absorption capacity. On the contrary, the cycle stability of the as-cast alloys obviously improves with the Sm content increasing, which can be attributed to the facilitated corrosion resistance by Sm substituting.

Key words: La-Mg-Ni based alloy; hydrogen storage properties; enthalpy change; entropy change; electrochemical performances

Hydrogen storage alloy is widely used as a negative electrode material of Ni/MH secondary battery from the perspective of environmental friendliness, safety, and high capacity [1,2]. The development of hydrogen storage materials is of great importance for application in the Ni/MH secondary battery system. Rare-earth based AB_5-type alloys have been commercialized successfully, but their low capacity limits extensive application [3,4]. So looking for new hydrogen storage materials attracts great attension. Recently, RE-Mg-Ni based alloys are considered as the promising hydrogen storage alloys in view of the higher discharge capacity compared with AB_5-type alloys [5-7]. Zhang et al. studied the electrochemical hydrogen storage characteristics of $La_{0.8-x}Pr_xMg_{0.2}Ni_{3.35}Al_{0.1}Si_{0.05}$ (x = 0~0.4) alloys and found that the alloys after annealing possess large discharge capacity (about 389.7 mAh/g) than $LaNi_5$ type alloys and cycle stability has a great improvement by Pr substitution and annealing treatment [8]. In order to seek a good balance between higher hydrogen storage capacity and long cycle life, much interest is focused on hydriding properties of AB_2-type $AMgNi_4$ alloys and the structure of $LaMgNi_4$ alloy was studied intensively. Kadir et al.[9] prepared $AMgNi_4$ (A = Ca, La, Ce, Pr, Nd, Y) alloys, and found that these compounds have a cubic $MgSnCu_4$ ($AuBe_5$ type) structure, which is an ordered superstructure between C36 type ($MgNi_2$) and C15 type ($MgCu_2$) Laves phase. Recently, Aono et al.[10] synthesized ternary compound $YMgNi_4$ with C15b($AuBe_5$)-type Laves phase structure and found that it has a suitable temperature range for hydrogen storage and lower dehydrogenization temperature; however, the maximum hydrogen content is about 1.05 wt%. Then Guénée et al.[11] studied the ternary compounds $LaMgNi_4$ and $NdMgNi_4$ alloys, and a hydrogen uptake of 5 H/f.u. at 8×10^5 Pa pressure and 326 K was observed. Wang et al. prepared $LaMgNi_4$ type alloys by mechanical ball milling, and the maximum discharge capacity can reach 400

Received date: August 14, 2015
Foundation item: National Natural Science Foundations of China (51161015, 51371094); Natural Science Foundation of Inner Mongolia, China (2011ZD10)
Corresponding author: Zhang Yanghuan, Ph. D., Professor, Department of Functional Material Research, Central Iron and Steel Research Institute, Beijing 100081, P. R. China, Tel: 0086-10-62183115, E-mail: zhangyh59@sina.com

mAh/g[12,13]. Although many important results have been reported on the investigation of the synthesis and structure of Re-Mg-Ni system alloys, the study on the electro-chemical properties is not so intensive and systemical for the $LaMgNi_4$ alloys. In the other hand, element substitution is an effective way to improve the hydrogen storage properties. So in the present work, we used rare earth Sm to substitute La and $La_{1-x}Sm_xMgNi_{3.6}Co_{0.4}$ (x = 0 ~ 0.4) electrode alloys were prepared and the gaseous and electro- chemical hydrogen storage properties as well as thermo- dynamic performances of the alloys were investigated.

1 Experiment

The experimental alloys with a chemical composition of $La_{1-x}Sm_xMgNi_{3.6}Co_{0.4}$ (x = 0~0.4) were prepared by a vacuum induction furnace in helium atmosphere under a pressure of 0.04 MPa. For convenience, the alloys were denoted with Sm content as Sm_0, Sm_1, Sm_2, Sm_3 and Sm_4, when x = 0, 0.1, 0.2, 0.3, 0.4. A slight excess of La, Sm, and Mg over-composition was needed to compensate for evaporative loss during the preparation. Then parts of the prepared ingots were mechanically crushed and ground into powder with a size of about 45 μm. The phase composition and structures of the alloys were characterized using XRD. The morphologies of the as-cast alloys were examined by SEM (Philips QUANTA 400). Pressure-composition (P-C-T) isotherms were measured at temperatures of 323, 348, 373 K and a pressure of 3 MPa by a Sieverts-type apparatus.

The experimental electrodes were prepared by mixing alloy powder and carbonyl nickel powder in the mass ratio of 1:4, and then the mixture was cold pressed at a pressure of 25 MPa into a pellet with a 15 mm diameter. The electrode pellets were immersed in 6 mol/L KOH solution for 24 h in order to wet the electrodes fully before the electrochemical measurement. Electrochemical measurements were performed at 303 K by a tri-electrode open cell, consisting of a working electrode (the metal hydride electrode), a sintered $Ni(OH)_2$/ NiOOH counter electrode and a Hg/HgO reference electrode, which were immersed in 6 mol/L KOH electrolyte. Charge/discharge tests were carried out by LAND battery testing system. In each cycle, the alloy electrode was charged for 7.5 h at 60 mA/g; after resting for 10 min, it was discharged at the same current density to cut-off voltage of –0.5 V. The cycle stability was tested by charging for 1.5 h at 300 mA/g and discharging at 300 mA/g to cut-off voltage of –0.5 V.

2 Results and Discussion

2.1 Microstructure of the as-received coating

The XRD patterns of $La_{1-x}Sm_xMgNi_{3.6}Co_{0.4}$ (x=0~0.4) alloys are displayed in Fig.1. It can be seen that all the alloys are composed of two phases, $LaMgNi_4$ as the major phase and $LaNi_5$ as the minor phase. Evidently, the diffraction peaks remain almost unchanged with increasing Sm content, which suggests that the substitution of Sm for La do not change the phase structures of all the alloys.

The crystal cell parameters of the major phase $LaMgNi_4$ of as-cast $La_{1-x}Sm_xMgNi_{3.6}Co_{0.4}$($x$=0~0.4) alloys were calculated by the Jade 6.0 software, and the results are listed in Table 1. It can be seen that the lattice constant a and the cell volume V of the $LaMgNi_4$ decrease with the increasing Sm content. The shrinkage of the cell volume should be caused by the substitution of Sm for La as the atomic radius of Sm (0.1804 nm) is smaller than that of La (0.1877 nm).

The SEM back scattered electron image and EDS pattern of the Sm_1 and Sm_3 alloys as representative examples of $La_{1-x}Sm_xMgNi_{3.6}Co_{0.4}$ (x = 0~0.4) alloys are shown in Fig.2. It is evident that the morphology of the as-cast alloy displays a typical dendritic structure, and there are two main areas with different colors in Fig.2. The EDS analyses show that the light grey and dark grey area correspond to $LaNi_5$ and $LaMgNi_4$ phase, respectively, which is consistent with the results obtained by XRD.

2.2 Gaseous hydrogen storage performances

Fig.3 shows the evolution of hydrogen storage capacity of the $La_{1-x}Sm_xMgNi_{3.6}Co_{0.4}$($x$=0~0.4) alloys with cycle number. It can be derived that the maximum hydrogen storage capacity (wt%) of the $La_{1-x}Sm_xMgNi_{3.6}Co_{0.4}$($x$=0~0.4) alloys is 1.859, 1.707, 1.585, 1.578 and 1.471. Clearly, the

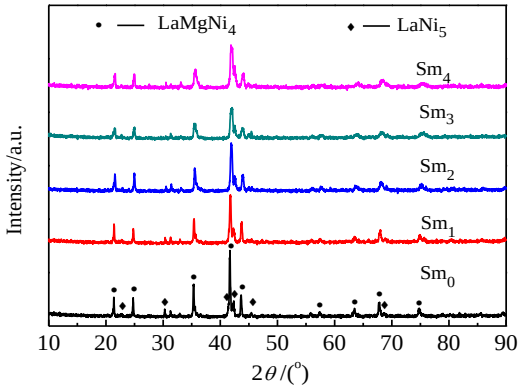

Fig.1 XRD patterns of the as-cast $La_{1-x}Sm_xMgNi_{3.6}Co_{0.4}$ (x = 0~0.4) alloys

Table 1 Crystal cell parameters of the major phase in $La_{1-x}Sm_x$ $MgNi_{3.6}Co_{0.4}$ (x=0~0.4)

Alloy	a/nm	V/×10^{-3}nm^3
Sm_0	0.7178	369.80
Sm_1	0.7158	366.81
Sm_2	0.7149	365.44
Sm_3	0.7145	364.85
Sm_4	0.7133	362.88

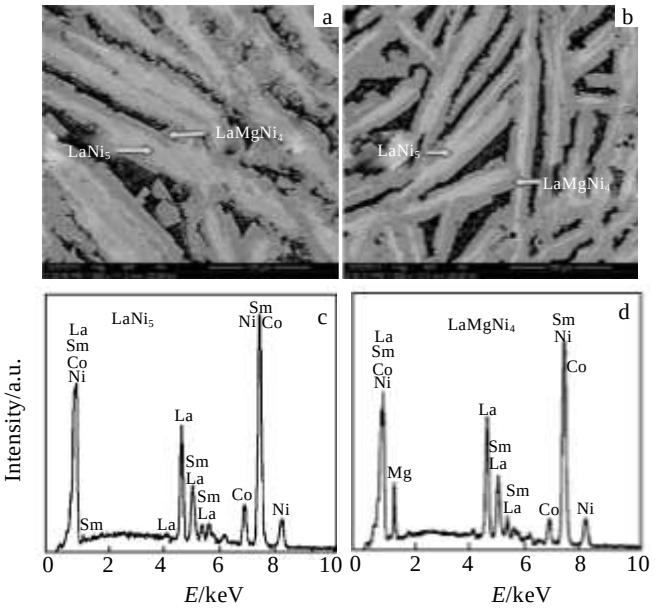

Fig.2 SEM back scattered electron imagess (a, b) and EDS patterns (c, d) for Sm_1 (a, c) and Sm_3 (b, d) alloys

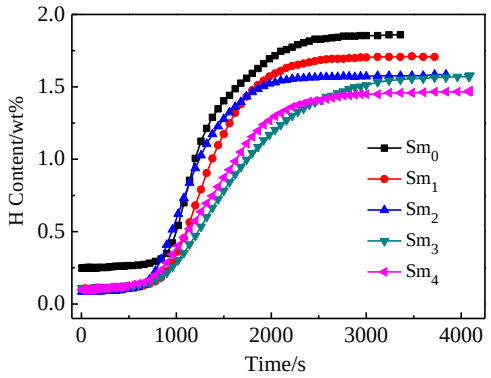

Fig.3 Evolution of hydrogen storage capacity of $La_{1-x}Sm_xMgNi_{3.6}Co_{0.4}$ (x=0~0.4) alloys with cycle number at 348 K

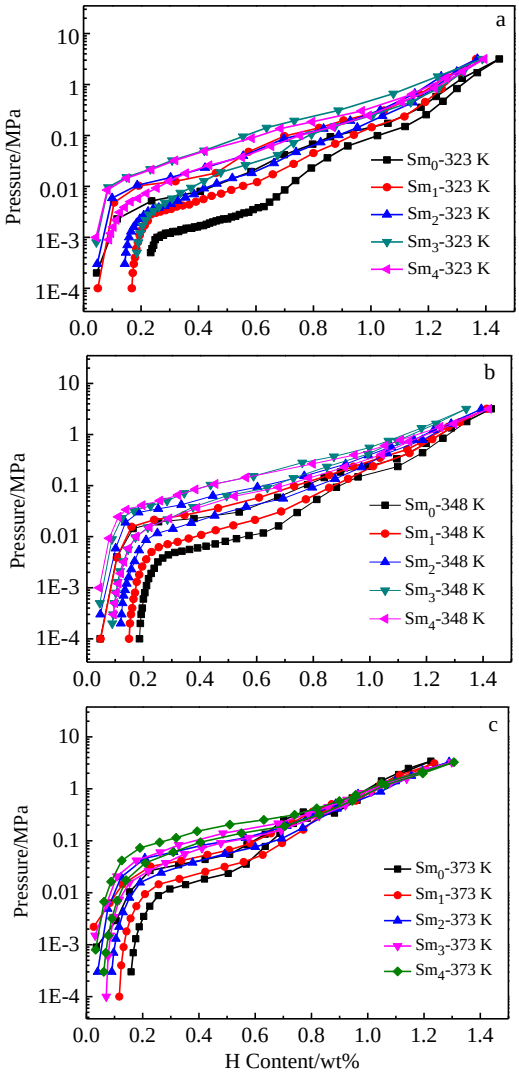

Fig.4 P-C-T curves of $La_{1-x}Sm_xMgNi_{3.6}Co_{0.4}$ (x=0~0.4) alloys at 323 K (a), 348 K (b), and 373 K (c)

maximum hydrogen storage capacity of $La_{1-x}Sm_xMgNi_{3.6}Co_{0.4}$ (x=0~0.4) alloys decreases with Sm content growing, which can be attributed to the shrinkage of cell volume. As in the hydrogen absorption progress, the hydrogen atoms enter into cell interstitial, so larger cell volume provides more space for hydrogen; hence higher hydrogen capacity is obtained.

The thermodynamics properties of the alloys can be studied through measuring the P-C-T curves at different temperatures. Fig.4 shows the P-C-T curves of the $La_{1-x}Sm_xMgNi_{3.6}Co_{0.4}$ (x = 0~0.4) alloys at 323, 348 and 373 K. It can be seen that there is a flat plateau around 0.01 ~ 0.1 MPa in every P-C-T curve, corresponding to the absorption/ desorption pressure plateaus of $LaMgNi_4$ hydride. With the increasing of Sm substitution, the plateau pressure for $LaNi_5$ hydride becomes less obvious. The plateau pressure goes up with increasing the Sm content at all three temperatures, indicating that the substitution of Sm for La decreases the stability of hydride, for which the decreased cell volume resulting from substituting La with Sm is basically responsible. On the other hand, the pressure plateau is closely related with the enthalpy changes of the hydride. So enthalpy and entropy changes of hydrogen absorption process are discussed in the next section.

2.3 Enthalpy and entropy changes of hydrogen absorption

The enthalpy and entropy changes as the thermodynamic parameters of the hydride can be calculated by the Van't Hoff plot:

$$\ln\frac{P}{P^{\Theta}}=\frac{\Delta H}{RT}-\frac{\Delta S}{R} \quad (1)$$

where, P is the equilibrium pressure (MPa), P^{Θ} is the standard atmosphere pressure (MPa), R is the gas constant (8.314 J $(K/mol)^{-1}$), and T is temperature (K).

According to the Van't Hoff plot, the enthalpy change ΔH and entropy change ΔS of the alloy hydride in absorption could be obtained from the slope and intercept of the plot shown Fig.5. The calculated ΔH and ΔS are listed in Table 2. It can be seen in Table 2 that the absolute value of the enthalpy change ΔH decreases with the Sm content increasing, so the pressure plateau of the $La_{1-x}Sm_xMgNi_{3.6}Co_{0.4}$ (x = 0~0.4) alloys becomes higher.

2.4 Electrochemical properties

The variation of the discharge capacity of $La_{1-x}Sm_xMgNi_{3.6}Co_{0.4}$ (x = 0 ~ 0.4) alloys with the cycle number is present in Fig.6. Apparently, all the alloy electrodes obtain their maximum discharge capacity at the first charge/discharge cycle, which is 347, 334.4, 321, 296 and 270.5 mAh/g. It is evident that the discharge capacity of the alloys decreases with the Sm content increasing, which shows a similar trend of the gaseous hydrogen capacity. As is well-known, the discharge capacity of the alloy is closely associated with the cell volume, namely the larger the cell volume is, the higher the discharge capacity of the alloy will be. Hence, we think that the decreased cell volume by Sm substitution is principally responsible for the reduction of the discharge capacity incurred by such substitution.

Fig.7 describes the cyclic stability of the alloy electrodes during 300 charge/discharge cycles. The cycle stability of the alloy electrode can be signified by the capacity retaining rate

Table 2 Calculated ΔH and ΔS of the major phase of $La_{1-x}Sm_xMgNi_{3.6}Co_{0.4}$ (x = 0~0.4) in absorption

Alloy	ΔH/kJ mol^{-1}	ΔS/J (mol/K)$^{-1}$
Sm_0	−40.37	−101.9
Sm_1	−31.30	−79.02
Sm_2	−30.26	−78.43
Sm_3	−28.12	−77.93
Sm_4	−26.99	−77.56

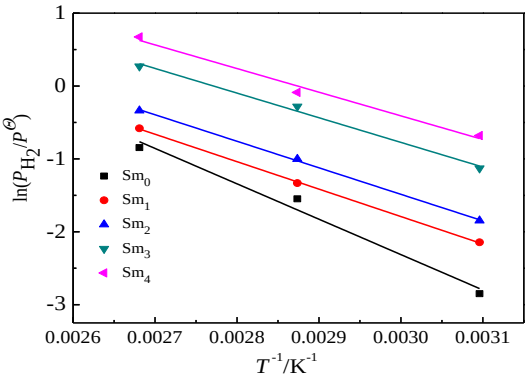

Fig.5 Fitting lines for ΔH and ΔS of $LaMgNi_4$ hydride in hydrogen absorption process

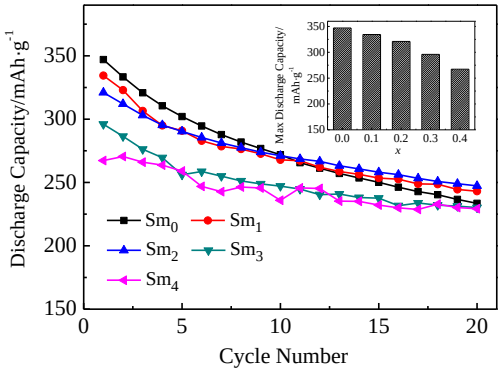

Fig.6 Evolution of the discharge capacity of the $La_{1-x}Sm_xMgNi_{3.6}Co_{0.4}$ (x=0~0.4) alloys with the cycle number

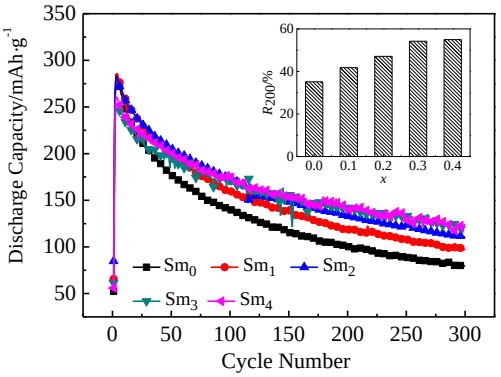

Fig.7 Cyclic stability of the alloy electrodes during 300 charge/discharge cycles

(R_n), being defined as $R_n=C_n/C_{max}\times100\%$, where C_{max} is the maximum discharge capacity while C_n is the discharge capacity at the nth charge-discharge cycle with a current density of 300 mA/g. The relationship between the R_{200} (n = 200) values of the alloys and the Sm content are inserted in Fig.7. R_{200} value is enhanced from 35.14% to 54.97% by increasing Sm content from 0 to 0.4, which indicates that Sm substitution facilitates for the cyclic stability.

The degradation of discharge capacity of alloys during charge/discharge cycling can be explained by the hydrogenation /dehydrogenation progress. Taking Sm_4 alloy after 300 charge/ discharge cycles as a representative example, a number of microscopic cracks appear on the surface of the alloy which can be seen clearly from Fig.8. It is well known that hydrogenation and dehydrogenation inevitably engenders the expansion and contraction of the cell volume [14-16], which enables the lattices of the alloy to generate internal stress. So microscopic cracks emerge to release such stress, hence inducing pulverization. On the other hand, La and Mg is very easy to corrode in the corrosive electrolyte, so Sm substitution for La improves anti-corrosion. The contribution of the Sm substitution to the cycle stability of the alloy is considered to be most likely associated with the facilitated corrosion resistance by Sm substituting.

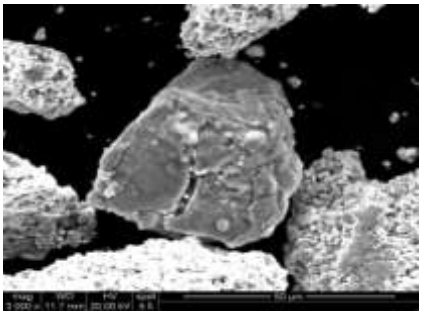

Fig.8 SEM image of Sm_4 alloy after 300 charge/discharge cycles

3 Conclusions

1) The as-cast $La_{1-x}Sm_xMgNi_{3.6}Co_{0.4}$ (x = 0~0.4) alloys were prepared by a vacuum induction furnace. All the alloys are composed of $LaMgNi_4$ and $LaNi_5$, and the substitution of Sm for La decreases the lattice constant a and cell volume V without altering the phase composition of the alloys.

2) Both the gaseous and electrochemical capacities decrease with increasing of the Sm content. Furthermore, the substitution of Sm for La gives rise to the plateau pressure of the alloys going up, which means a decrease in thermal stability of the hydride and hence the absolute value of the enthalpy change ΔH decreases with the Sm content increasing.

3) Capacity retaining rate (R_{200}) of the alloys is enhanced from 35.14% to 54.97% by the Sm content increasing from x = 0 to x = 0.4.

References

1 Uehara I, Sakai T, Ishikawa H. *Journal of Alloys and Compounds*[J], 199, 253-254(1-2): 635

2 Sakintuna B, Lamari-Darkrim F, Hirscher M. *International Journal of Hydrogen Energy*[J], 2007, 32(9): 1121

3 Meli F, Zuttel A, Schlapbach L. *Journal of Alloys and Compounds*[J], 1993, 202(1-2): 81

4 Lichtenberg F, Kohler U, Fozler A *et al*. *Journal of Alloys and Compounds*[J], 1997, 253-254: 570

5 Kadir K, Sakai T, Uehara I. *Journal of Alloys and Compounds* [J], 1997, 257(1-2): 115

6 Kohno T, Yoshida H, Kawashima F *et al*. *Journal of Alloys and Compounds*[J], 2000, 311(2): L5

7 Dong Z W, Ma L Q, Wu Y M *et al*. *International Journal of Hydrogen Energy*[J], 2011, 36(4): 3016

8 Zhang Y H, Cai Y, Li B W *et al*. *Rare Metal Materials and Engineering*[J], 2013, 42(10): 1981

9 Kadir K, Noreus D, Yamashita I. *Journal of Alloys and Compounds*[J], 2002, 345(1-2): 140

10 Aono K, Orimo S, Fujii H. *Journal of Alloys and Compounds*[J], 2000, 309(1-2): L1

11 Guénée L, Favre-Nicolin V, Yvon K. *Journal of Alloys and Compounds*[J], 2003, 348(1-2): 129

12 Wang Z M, Zhou H Y, Gu Z F *et al*. *Journal of Alloys and Compounds*[J], 2004, 377(1-2): L7

13 Wang Z M, Ni C Y, Zhou H Y *et al*. *Materials Characterization*[J], 2008, 59(4): 422

14 Liu Y F, Pan H G, Yue Y J *et al*. *Journal of Alloys and Compounds*[J], 2005, 395(1-2): 291

15 Liu Y F, Pan H G, Gao M X *et al*. *International Journal of Hydrogen Energy*[J], 2008, 33(1): 124

16 Zhang Y H, Hu F, Li Z G *et al*. *Journal of Alloys and Compounds*[J], 2011, 509(2): 294

铸态 $La_{1-x}Sm_xMg_{3.6}Co_{0.4}$ (x = 0~0.4)合金的贮氢性能

翟亭亭[1,2]，杨 泰[1]，袁泽明[1]，许 胜[1]，张羊换[1]

(1. 钢铁研究总院，北京 100081)

(2. 东北大学，辽宁 沈阳 110819)

摘 要：采用真空感应熔炼方法制备了 $La_{1-x}Sm_xMgNi_{3.6}Co_{0.4}$ (x = 0~0.4)合金，并系统研究了 Sm 替代 La 对合金相结构、形貌、以及贮氢性能的影响。利用 XRD 和 SEM 分析了合金的相结构。结果表明，合金包含 $LaMgNi_4$ 和 $LaNi_5$ 两相；$La_{1-x}Sm_xMgNi_{3.6}Co_{0.4}$ (x=0~0.4) 系列合金在 348 K，3 MPa 下的气态吸氢量(质量分数，%)随着 Sm 添加呈现逐渐降低的趋势，分别为 1.859、 1.707、1.585、1.578、1.471；合金的 P-C-T 曲线显示 $LaMgNi_4$ 相在吸放氢时有平坦的平台压，同时通过在 323，348，373 K 下对合金 P-C-T 曲线的研究表明，$La_{1-x}Sm_xMgNi_{3.6}Co_{0.4}$ (x= 0~0.4)合金中 $LaMgNi_4$ 相在吸氢过程中的焓变在 x = 0 时为−40.37 kJ/mol，随着 Sm 替代量增加到 x = 0.4，焓变降到了−26.99 kJ/mol。而熵变也从 x=0 时的−101.9 J (mol/K)$^{-1}$ 降到了 x = 0.4 时的−77.56 J (mol/K)$^{-1}$；$La_{1-x}Sm_xMgNi_{3.6}Co_{0.4}$ (x=0~0.4)合金的电化学合金测试表明，最大放电容量随着 Sm 替代量的增加从 347 mAh/g 降到了 270.5 mAh/g，但是合金的循环稳定性随着 Sm 替代的增加得到了很大的提高。

关键词：La-Mg-Ni 系合金；贮氢性能；焓变；熵变；电化学性能

作者简介：翟亭亭，女，1986 年生，博士生，钢铁研究总院功能材料所，北京 100081，电话：010-62183115，E-mail：mailzhaitt@126.com